Journal of Alloys and Compounds 509 (2011) 6190–6195

Contents lists available at ScienceDirect

Journal of Alloys and Compounds

journal homepage: www.elsevier.com/locate/jallcom

Isothermal section of the Al–Dy–Zr ternary system at 773 K

Xiaoli Yuan [a], Libin Liu [a,b,c,*], Gemei Cai [a,b,c], Hong Bo [a], Fuyong Cao [a], Feng Zheng [a,b,c]

[a] School of Materials Science and Engineering, Central South University, Changsha, Hunan, 410083, PR China
[b] Education Ministry Key Laboratory of Non-ferrous Materials Science and Engineering, Central South University, Changsha, 410083, PR China
[c] Science Center for Phase Diagram & Materials Design and Manufacture, Central South University, Changsha, Hunan 410083, PR China

ARTICLE INFO

Article history:
Received 12 October 2010
Received in revised form 16 February 2011
Accepted 17 February 2011
Available online 23 February 2011

Keywords:
Phase diagrams
Metals and alloys
X-ray diffraction
Scanning electron microscopy

ABSTRACT

The phase relations in the Al–Dy–Zr ternary system at 773 K have been investigated by X-ray powder diffraction (XRD) and scanning electron microscope (SEM) with energy disperse X-ray spectroscopy (EDX) in backscattered electron imaging (BSE) modes. The isothermal section at this temperature is featured with 17 single-phase regions, 32 two-phase regions and 16 three-phase regions. Besides, the ternary compound $Al_{30}Dy_7Zr_3$ has been confirmed to be existed. The maximum solid solubility of Zr in $AlDy_2$, Al_2Dy_3, AlDy, Al_2Dy and Al_3Dy at 773 K is determined to be 11.5 at.%, 7.8 at.%, 2.4 at.%, 22.5 at.% and 2.5 at.%, respectively.

1. Introduction

Aluminum alloys find potential application in automobile and aerospace industries [1–3] for their high strength to weight ratio. The microstructure and properties of them can be strongly affected by adding small amounts of transition elements such as Zr, Mn and Cr, etc. [4–6]. As a very important alloying element, Zr optimizes various aspects of Al alloys like refining grains, inhibiting re-crystallization and improving stress corrosion cracking resistance [7,8]. Formation of Al_3Zr precipitates in aluminum alloys especially in those for aerospace applications has gotten sufficient investigations [9,10]. Not easily to be broken down by dislocation cutting, the strong covalence Al–Zr bond in Al_3Zr can hinder dislocation moving. High strength, good corrosion resistance and low capture cross section for thermal neutrons of $AlZr_3$ compound indicates its broad prospect in the nuclear industry [11].

Substantial interest in Al–RE (RE = rare earth) alloys has been aroused for years [12–15] due to their special physical properties and possibility of commercial application. Properties of these alloys are strongly related with the formation of the inter-metallic compounds. For example, metallic compounds of Al_3Sm or Al_3Dy can significantly lower the resistivity of the alloy [16] and Al_3Sc plays an important role in improving the strength of Al–Sc alloy [17]. Therefore, it is necessary to investigate the phase diagram of RE–Al–Zr systems to develop alloys with required properties. Recently, RE–Al–Zr (RE = Y, La, Ce, Pr, Ho) phase diagram [18–22] are reported. Dy is a significant magnetic element in lanthanon, benefiting the mechanical properties of Al alloy omnifariously [23]. However, very few reports can be found on the Dy–Al–Zr ternary system.

According to Refs. [24] and [25], there are five compounds, i.e., Al_3Dy, Al_2Dy, AlDy, Al_2Dy_3 and $AlDy_2$ in the Al–Dy binary phase diagram and eight phases, i.e., Al_3Zr, Al_2Zr, Al_3Zr_2, AlZr, Al_3Zr_4, Al_2Zr_3, $AlZr_2$ and $AlZr_3$ in the Al–Zr phase diagram at 773 K, respectively. No binary compound was found in the Zr–Dy phase diagram. Tyvanchuk and Protsyk [27] determined the isothermal section of the Al-rich corner of Al–Zr–Dy ternary system at 773 K and identified the existence of one compound $Al_{30}Dy_7Zr_3$ [27] in 1982. But in order to show complete phase relationship of this system, we investigated the whole isothermal section at 773 K to provide information for materials design and calculation of phase diagrams. Crystallographic data of the phases in the Al–Dy–Zr system [27–29] are given in Table 1.

2. Experimental procedures

In this work, the alloy buttons (each weight 2 gm) were prepared in an electric arc furnace under pure argon atmosphere with a water-cooled cooper crucible. The purity of the starting materials Al, Dy and Zr used in this work was all 99.99 wt.%. Titanium was used as an oxygen getter during the melting process. All samples were melted four times in order to achieve complete fusion and homogeneous composition. The weight loss is less than 1% after melting for most of the buttons. All the melted alloy samples were sealed in evacuated quartz tubes for homogenization. The homogenization temperature was determined by differential thermal analysis (DTA) or based on previous work of the three binary phase diagrams [24–26]. Most samples were annealed at 873 K for 360 h and then cooled at a

* Corresponding author at: School of Materials Science and Engineering, Central South University, Lushan Street 105#, Changsha, Hunan, 410083, PR China.
Tel.: +86 0731 88877732; fax: +86 0731 88876692.
E-mail address: pdc@mail.csu.edu.cn (L. Liu).

0925-8388/$ – see front matter © 2011 Published by Elsevier B.V.
doi:10.1016/j.jallcom.2011.02.079

Table 1
Crystallographic data of intermediate phases in the Al–Dy–Zr system.

Compound	Space group	Lattice parameters (nm)			Reference
		a	*b*	*c*	
α-Al_3Dy	*$P6_3/mmc$*	0.6091	–	0.9533	[28]
β-Al_3Dy	*$R\bar{3}m$*	0.6070	–	3.594	[28]
Al_2Dy	*$Fd\bar{3}m$*	0.778	–		[28]
AlDy	*Pmma*	0.5570	0.5801	1.1272	[28]
Al_2Dy_3	*P42/mnm*	0.817	–	0.754	[28]
$AlDy_2$	*Pnma*	0.654	0.508	0.940	[28]
Al_3Zr	*I4/mmm*	0.4005	–	1.7285	[29]
Al_2Zr	*$p6_3/mmc$*	0.52824	–	0.87482	[29]
Al_3Zr_2	*Fdd2*	0.9601	1.3906	0.5574	[29]
AlZr	*Cmcm*	0.3353	1.0866	0.4266	[29]
Al_3Zr_4	*$p\bar{6}$*	0.5433	–	0.5390	[29]
Al_2Zr_3	*$p4_2/mmm$*	0.7630	–	0.6998	[29]
$AlZr_2$	*$p6_3/mmc$*	0.4894	–	0.5928	[29]
$AlZr_3$	*$Pm\bar{3}m$*	0.43917	–	–	[29]
$Al_{30}Dy_7Zr_3$	*$Pm\bar{3}m$*	0.42	–	–	[27]

Table 2
Details of the three-phase regions in the Al–Dy–Zr system at 773 K.

Alloy no.	Nominal composition (at.%)	Phase composition
1	Al84Dy13Zr3	$Al + Al_{30}Dy_7Zr_3 + Al_3Dy$
2	Al86Dy4Zr10	$Al + Al_{30}Dy_7Zr_3 + Al_3Zr$
3	Al73Dy22Zr5	$Al_3Dy + Al_2Dy + Al_{30}Dy_7Zr_3$
4	Al72Dy10Zr18	$Al_{30}Dy_7Zr_3 + Al_2Dy + Al_3Zr$
5	Al70Dy5Zr25	$Al_2Dy + Al_2Zr + Al_3Zr$
6	Al65Dy5Zr30	$Al_3Zr_2 + Al_2Zr + Al_2Dy$
7	Al60Dy25Zr15	$Al_3Zr_2 + AlDy + Al_2Dy$
8	Al54Dy22Zr24	$Al_3Zr_2 + AlDy + AlZr$
9	Al48Dy20Zr32	$Al_3Zr_4 + AlZr + AlDy$
10	Al43Dy10Zr47	$Al_2Zr_3 + Al_3Zr_4 + AlDy$
11	Al42Dy38Zr20	$Al_2Zr_3 + AlDy + Al_2Dy_3$
12	Al38Dy32Zr30	$AlZr_2 + Al_2Zr_3 + Al_2Dy_3$
13	Al37Dy45Zr18	$AlZr_2 + AlDy_2 + Al_2Dy_3$
14	Al30Dy35Zr35	$AlDy_2 + AlZr_2 + Dy$
15	Al20Dy30Zr50	$AlZr_2 + AlZr_3 + Dy$
16	Al10Dy20Zr70	$AlZr_3 + Dy + Zr$

rate of 3 K/h to 773 K and maintained for 720 h. Finally, they were quenched in water.

All the sample buttons were ground into powder for powder X-ray diffraction (XRD) analysis. The XRD analysis was performed on a Rigaku D/Max 2500 V diffractometer with Cu radiation and graphite monochromator operated at 40 kV and 200 mA. The Material Data Inc. software Jade 5.0 and powder diffraction file (PDF release 2004) were used for phase identification. Scanning electron microscopy (SEM) with energy dispersive X-ray analysis (EDX) was used for microstructure and elemental analysis. By all these means, the phase relationships in the Al–Dy–Zr system at 773 K were determined.

3. Results and discussion

3.1. Isothermal section

Based on the XRD, SEM and EDX analysis of all the samples, there is no new ternary compound in this system at 773 K. The existence of 13 binary compounds, namely Al_3Zr, Al_2Zr, Al_3Zr_2, AlZr, Al_3Zr_4, Al_2Zr_3, $AlZr_2$, $AlZr_3$, Al_3Dy, Al_2Dy, AlDy, Al_2Dy_3, $AlDy_2$, and one ternary compound $Al_{30}Dy_7Zr_3$, have been confirmed. The isothermal section of the Al–Dy–Zr ternary system at 773 K is shown in Fig. 1. It consists of 17 single-phase regions, 32 two-phase regions and 16 three-phase regions. The 17 single-phase regions are: A($Al_{30}Dy_7Zr_3$), B(Al), C(Dy), D(Zr), E(Al_3Zr), F(Al_2Zr), G(Al_3Zr_2), H(AlZr), I(Al_3Zr_4), J(Al_2Zr_3), K($AlZr_2$), L($AlZr_3$), M(Al_3Dy), N(Al_2Dy), O(AlDy), P(Al_2Dy_3), and Q($AlDy_2$), respectively. The 32 two-phase regions are: A + B, A + E, A + M, A + N, B + E, B + M, C + D, C + K, C + L, C + Q, D + L, E + F, E + N, F + G, F + N, G + H, G + N, G + O, H + I, H + O, I + J, I + O, J + K, J + O, J + Q, K + L, K + P, K + Q, M + N, N + O, O + P, P + Q. The 16 three-phase regions are: A + B + E, A + B + M, A + E + N, A + M + N, C + D + L, C + K + L, C + K + Q, E + F + N, F + G + N, G + H + O, G + O + N, H + I + O, I + J + O, J + O + P, J + K + P, K + P + Q, respectively. Phase constitutions of the three-phase regions and compositions of the typical alloys are given in Table 2.

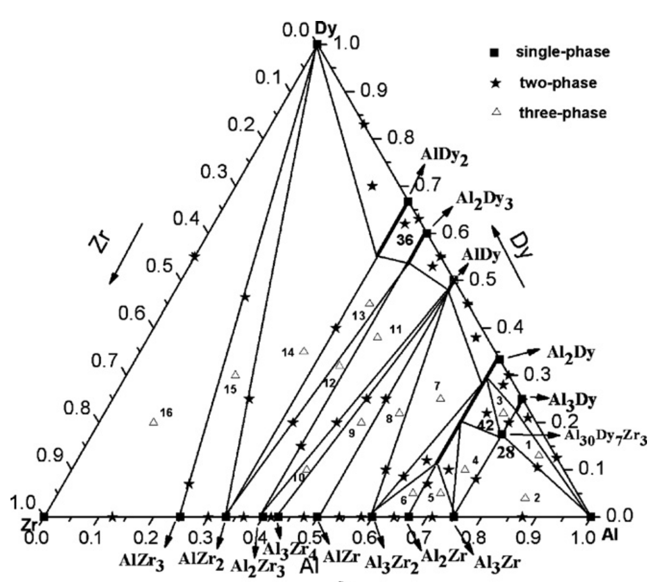

Fig. 1. Isothermal section of the Al–Dy–Zr ternary system at 773 K.

The solid solubility ranges of all the single phases have been determined by using the phase-disappearing method and comparing the shift of the XRD pattern of the samples near to the compositions of the binary phases [30] together with scanning electron microscopy with energy dispersive X-ray analysis. The maximum solid solubility of Zr in $AlDy_2$, Al_2Dy_3, AlDy, Al_2Dy and Al_3Dy is found to be 11.5 at.%, 7.8 at.%, 2.4 at.%, 22.5 at.% and 2.5 at.%, respectively, at 773 K. The single phase extends parallel to the Dy–Zr line, which means that a certain amount of Dy atoms are replaced by Zr in these compounds. However, other intermediate compounds in this system do not have a remarkable solid solution at 773 K.

3.2. Phase analysis and solid solubility

In the Al–Dy–Zr ternary system, 13 binary compounds including Al_3Zr, Al_2Zr, Al_3Zr_2, AlZr, Al_3Zr_4, Al_2Zr_3, $AlZr_2$, $AlZr_3$, Al_3Dy, Al_2Dy, AlDy, Al_2Dy_3, $AlDy_2$ [24,25], and one ternary compound $Al_{30}Dy_7Zr_3$ [27] were reported. As there aren't any reported JCPDS PDF cards of intermediate compounds $AlDy_2$ and $Al_{30}Dy_7Zr_3$, we couldn't affirm the existence of $AlDy_2$ and $Al_{30}Dy_7Zr_3$ by directly comparing our experimental XRD patterns with the respective JCPDS PDF cards just as what we did in the identification of the other compounds. With the crystallographic data of $AlDy_2$ taken from Ref. [31] and that of $Al_{30}Dy_7Zr_3$ taken from Ref. [27], the XRD patterns of the compound $AlDy_2$ and $Al_{30}Dy_7Zr_3$ were calculated using the CaRIne program [32]. The results of XRD analysis of alloy samples are consistent with the respective JCPDS PDF cards and the calculated XRD pattern of $AlDy_2$ and $Al_{30}Dy_7Zr_3$.

As is shown in Fig. 2, the comparison of the experimental XRD pattern of 28# sample (75 at.% Al, 17.5 at.% Dy, 7.5 at.% Zr) and the calculated XRD pattern from [27] indicates the existence of phase $Al_{30}Dy_7Zr_3$. The XRD pattern of 42# sample (70 at.% Al, 22 at.% Dy, 8 at.% Zr) consists of two phases, i.e. Al_2Dy and $Al_{30}Dy_7Zr_3$, which means the existence of phases Al_2Dy and $Al_{30}Dy_7Zr_3$, and proves the presence of the two-phase region $Al_2Dy + Al_{30}Dy_7Zr_3$ as well (Fig. 3). The XRD pattern of 36# sample (35 at.% Al, 62 at.% Dy, 3 at.% Zr) indicates that the sample contains the phases of $AlDy_2$

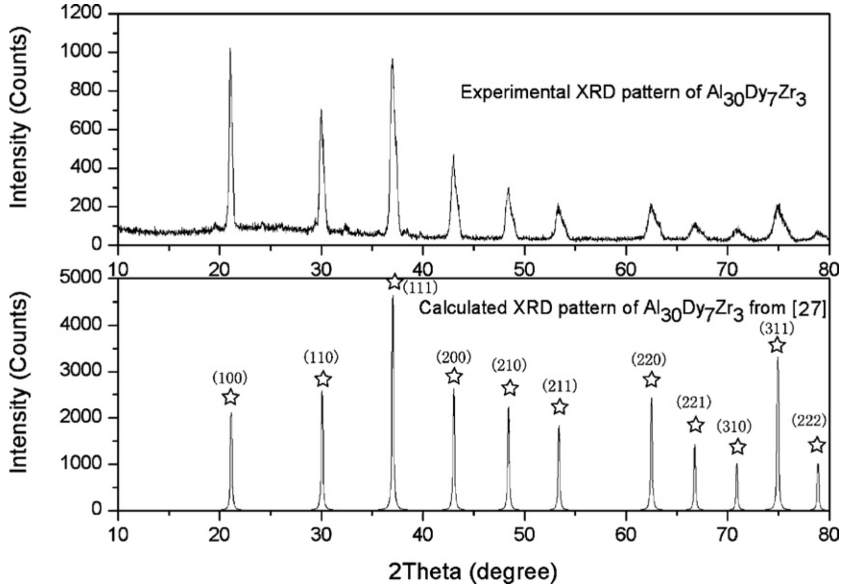

Fig. 2. Comparisons of experimental XRD pattern of 28# sample (75 at.% Al, 17.5 at.% Dy, 7.5 at.% Zr) and calculatde XRD pattern of $Al_{30}Dy_7Zr_3$ from [27].

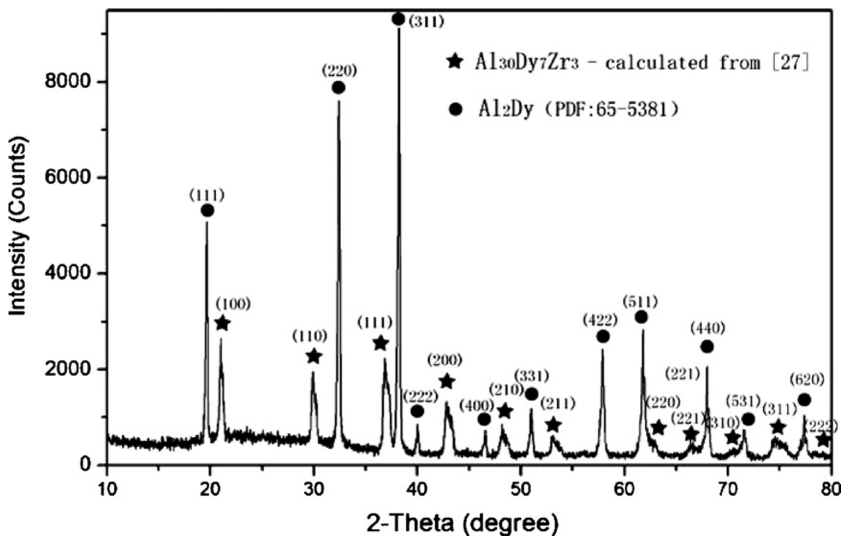

Fig. 3. XRD pattern of 42# sample (70 at.% Al, 22 at.% Dy, 8 at.% Zr) indicating the phase equilibrium of Al_2Dy and $Al_{30}Dy_7Zr_3$.

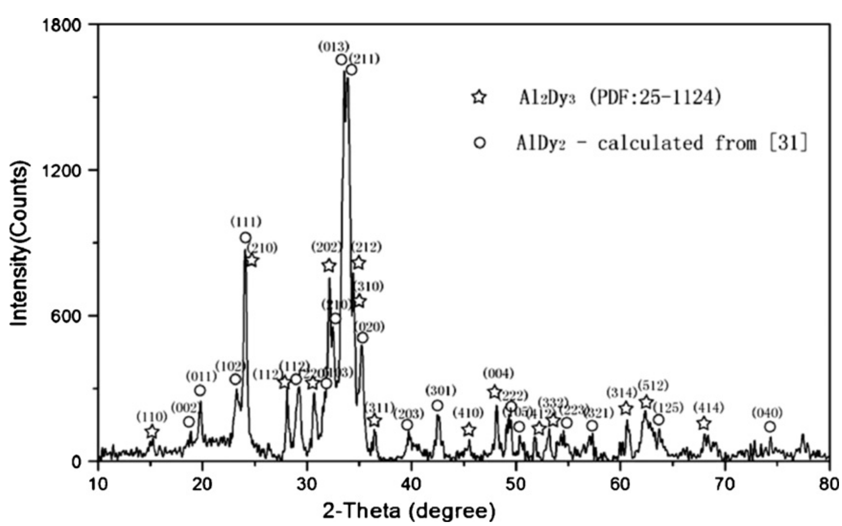

Fig. 4. XRD pattern of 36# sample (35 at.% Al, 62 at.% Dy, 3 at.% Zr) indicating the phase equilibrium of $AlDy_2$ and Al_2Dy_3.

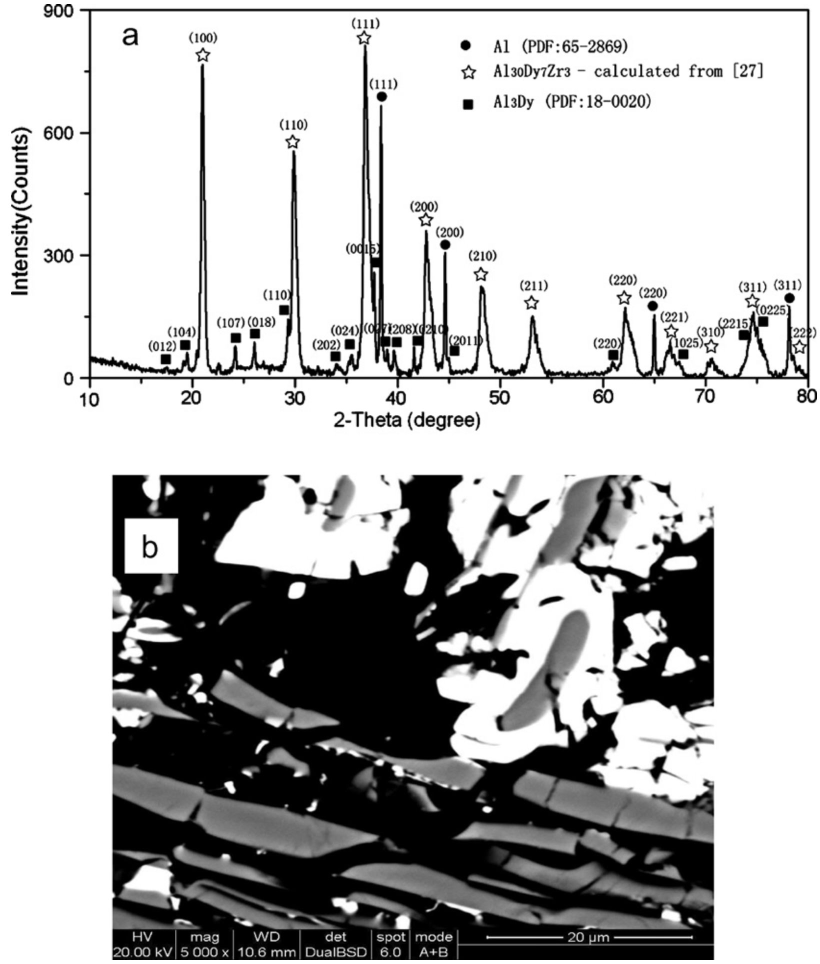

Fig. 5. (a) XRD pattern of #1 sample (84 at.% Al, 13 at.% Dy, 3 at.% Zr) indicating the phase equilibrium of Al, Al_3Dy and $Al_{30}Dy_7Zr_3$; (b) BSE image of #1 sample: Al (dark phase), Al_3Dy (light phase) and $Al_{30}Dy_7Zr_3$ (gray phase).

and Al_2Dy_3, which also confirms the existence of the two-phase region $AlDy_2 + Al_2Dy_3$ (Fig. 4).

In the Al-Dy system, Pop et al. [33] reported a hexagonal binary compound $Al_{17}Dy_2$ with the $Ni_{17}Th_2$ structure (space group $P6_3mmc$, $a = 1.1788$ nm, $c = 1.1322$ nm). In Zhou et al.'s work [34], a series of alloy samples in the Al-rich region of Al–Dy–Ti system were prepared, but they did not find the compound $Al_{17}Dy_2$, and Qin et al. [35] also got the same conclusion in their study of isothermal section of the Al–Dy–Ge ternary system at 673 K. In the present work, the equilibrated alloy #1(84 at.% Al, 13 at.% Dy and 3 at.% Zr) consists of three phases, i.e. Al, Al_3Dy and $Al_{30}Dy_7Zr_3$, as is shown in Fig. 5(a). The SEM result also shows the existence of three phases (Fig. 5(b)). From the EDX result, it can be seen that the light phase is Al_3Dy, the gray one $Al_{30}Dy_7Zr_3$, and the dark one Al. No evidence is found to confirm the existence of $Al_{17}Dy_2$, which is in accordance with the result of Zhou et al. [34] and Qin et al. [35].

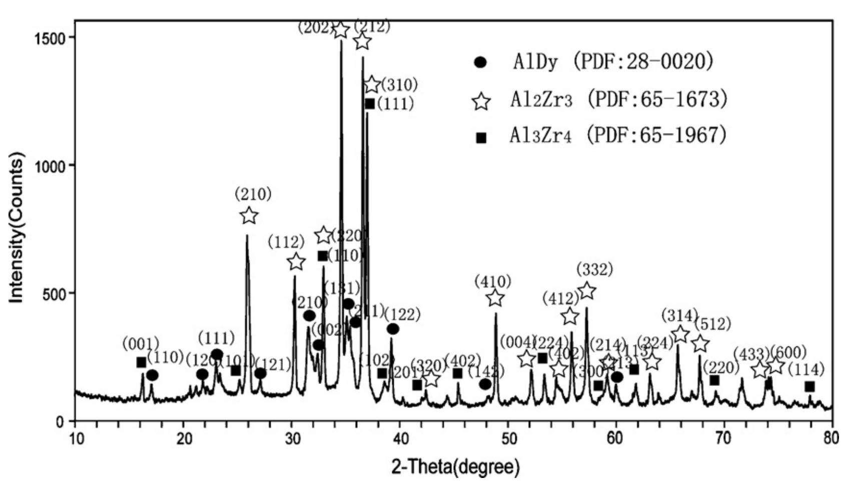

Fig. 6. XRD pattern of #10 sample (43 at.% Al, 10 at.% Dy, 47 at.% Zr) indicating the phase equilibrium of Al_2Zr_3, Al_3Zr_4 and AlDy.

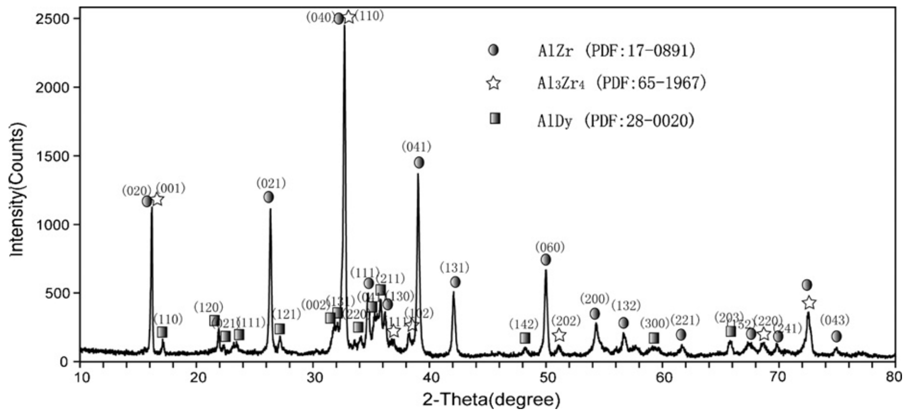

Fig. 7. XRD pattern of #9 sample (48 at.% Al, 20 at.% Dy, 32 at.% Zr) indicating the phase equilibrium of AlZr, Al_3Zr_4 and AlDy.

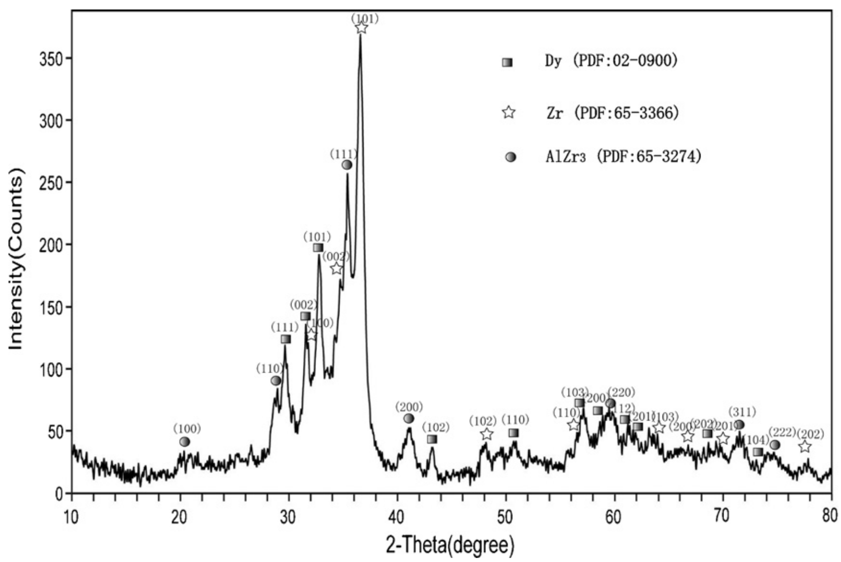

Fig. 8. XRD pattern of #16 sample (10 at.% Al, 20 at.% Dy, 70 at.% Zr) indicating the phase equilibrium of Dy, Zr and $AlZr_3$.

In the Al–Zr binary system, it is reported that the binary phase Al_3Zr_5 forms through the peritectic reaction L + Al_2Zr_3 ↔ Al_3Zr_5 at 1480 °C[36], which is stable in the temperature range of 1000–1480 °C but not under 1000 °C because of the eutectoid reaction Al_3Zr_5 ↔ $AlZr_2$ + Al_2Zr_3. In the present work, the XRD pattern of the #10 sample (43 at.% Al, 10 at.% Dy and 47 at.% Zr) indicates the existence of the three binary compounds i.e. Al_2Zr_3, Al_3Zr_4 and AlDy in the Al–Dy–Zr system (Fig. 6), which shows that there is no Al_3Zr_5 phase. Therefore, Al_3Zr_5 is considered to be a high temperature phase, which is in accordance with the result of Okamoto [36]. In Rigaud et al.'s work [37], the binary compound Al_4Zr_5 also underwent a high temperature transformation at about 1000 °C in Hu et al.'s work [20], the XRD pattern of the equilibrated alloy (Al:Zr = 4:5) had been analyzed and the result showed that this compound did not exist at 773 K. In this work, the XRD pattern of #9 sample (48 at.% Al, 20 at.% Dy and 32 at.% Zr) indicates the existence of the three binary compounds i.e. AlZr, Al_3Zr_4 and AlDy in the Al–Dy–Zr system (Fig. 7), showing that the compound Al_4Zr_5 does not exist at 773 K. This result is in accordance with that of Okamoto [36], Rigaud et al. [37] and Hu et al. [20].

In the Dy–Zr system, it has been confirmed that no binary compound exists [26]. In this work, the XRD pattern of the #16 sample (10 at.% Al, 20 at.% Dy and 70 at.% Zr) consists of the patterns of three phases, i.e. Dy, Zr and $AlZr_3$ (Fig. 8), which means that there is no binary compound at 773 K.

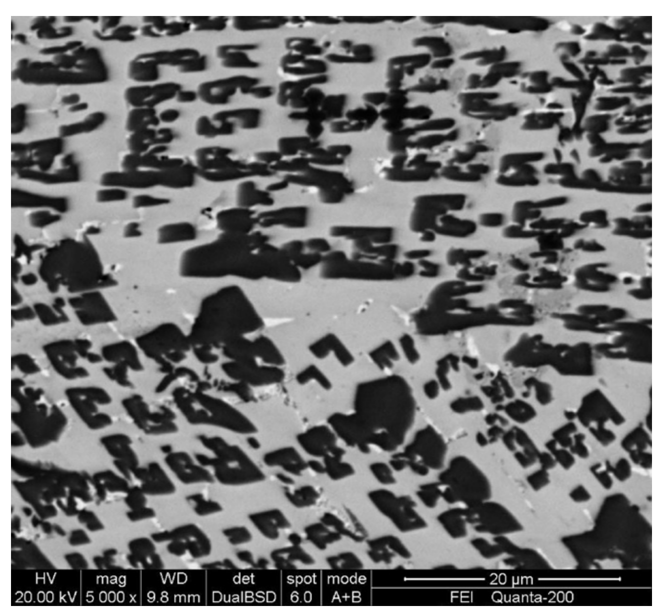

Fig. 9. BSE image of #14 sample (30 at.% Al, 35 at.% Dy, 35 at.% Zr) indicating the three phase equilibrium of Dy (light phase), $AlZr_2$ (dark phase), and $AlDy_2$ (gray phase).

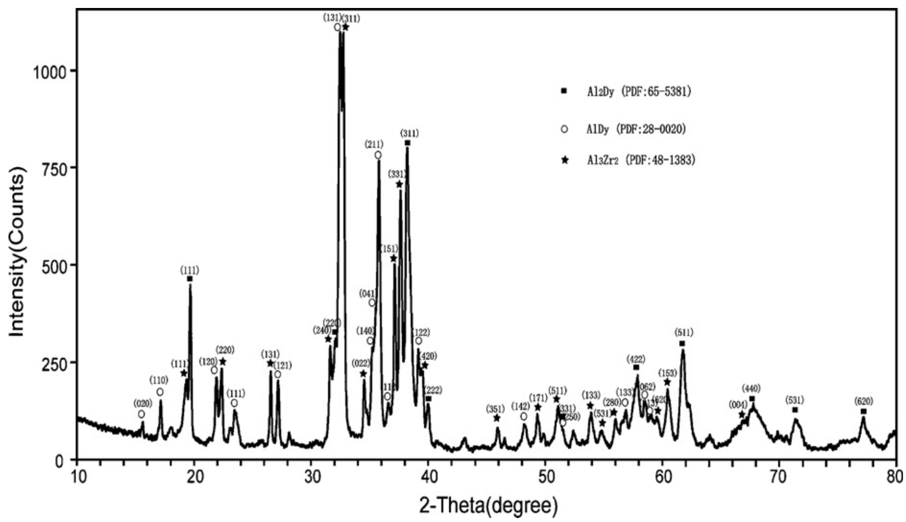

Fig. 10. XRD pattern of #7 sample (60 at.% Al, 25 at.% Dy, 15 at.% Zr) indicating the phase equilibrium of Al_3Zr_2, Al_2Dy and AlDy.

To find possible ternary compounds in the region adjoining the $AlDy_2$ + Dy two-phase region, we prepared a set of samples. The XRD results of these samples show the existence of a three-phase region of $AlDy_2$ + $AlZr_2$ + Dy. The SEM micrograph of the #14 sample (30 at.% Al, 35 at.% Zr, 35 at.% Dy), as shown in Fig. 9, clearly show the three-phase equilibrium, indicating that there are no new ternary compounds in this region. Similarly, the XRD patterns of the #7 sample (60 at.% Al, 25 at.% Dy, 15 at.% Zr), as shown in Fig. 10, consisting a three phase region of AlDy + Al_2Dy + Al_3Zr_2, also indicate that there are no new ternary compounds in the region adjoining the AlDy + Al_2Dy two phase region.

4. Conclusions

By comparing and analyzing the XRD patterns of all the equilibrated samples, the phase relations of the Al–Dy–Zr ternary system at 773 K have been determined. The 773 K isothermal section consists of 17 single-phase regions, 32 two-phase regions and 16 three-phase regions. The Al_3Zr_5 and Al_4Zr_5 compounds are not found, whereas the existence of the ternary compound $Al_{30}Dy_7Zr_3$ has been confirmed.

Acknowledgement

This work was financially supported by National Science Foundation of China (Grant Nos. 50971136, 50771106 and 50731002) and Key Project of Chinese Ministry of Education (No. 109122).

References

[1] J.C. Williams, E.A. Starke, Acta Mater. 51 (19) (2003) 5775–5799.
[2] J. Wloka, T. Hack, S. Virtanen, Corros. Sci. 49 (3) (2007) 1437–1449.
[3] M. Rajamuthamilselvan, S. Ramanathan, J. Alloys Compd. 509 (2011) 948–952.
[4] M. Sha, S. Wu, G. Zhong, P. An, J. Alloys Compd. 509 (2011) 252–257.
[5] X.M. Li, M.J. Starink, J. Alloys Compd. 509 (2011) 471–476.
[6] G.W. Qin, Y.P. Ren, W. Huang, S. Li, W.L. Pei, J. Alloys Compd. 507 (2010) 410–413.
[7] Z.Y. Ma, R.S. Mishra, Scripta Mater. 53 (2005) 75–80.
[8] T.V. Atamanenko, D.G. Eskin, M. Sluiter, L. Katgerman, J. Alloys Compd. 509 (2011) 57–60.
[9] E. Clouet, A. Barbu, L. Laé, G. Martin, Acta Mater. 53 (2005) 2313–2325.
[10] L. Li, Y.D. Zhang, C. Esling, H.X. Jiang, et al., J. Cryst. Growth 316 (2011) 172–176.
[11] A. Laik, K. Bhanumurthy, G.B. Kale, Intermetallics 12 (2004) 69–74.
[12] J. Sarkar, S. Saimoto, B. Mathew, P.S. Gilman, J. Alloys Compd. 479 (2009) 719–725.
[13] R.A. Karnesky, M.E. Dalen, D.C. Dunand, et al., Scripta Mater. 55 (2006) 437–440.
[14] F. Rosalbino, S. Delsante, G. Borzone, E. Angelini, Corros. Sci. 52 (2010) 322–326.
[15] Y.C. Tsai, C.Y. Chou, S.L. Lee, et al., J. Alloys Compd. 487 (2009) 157–162.
[16] S. Takayama, N. Tsutsui, Thin Solid Films 289 (1996) 289–294.
[17] Y. Ye, P. Li, L. Novikov, V. Avilkina, L. He, Acta Mater. 58 (2010) 2520–2526.
[18] J. She, Y.Z. Zhan, Z.H. Hu, et al., J. Alloys Compd. 497 (2010) 118–120.
[19] D. Peng, Y.Z. Zhan, J. She, J. Alloys Compd. 507 (2010) 62–66.
[20] Z.H. Hu, Y.Z. Zhan, J. She, et al., J. Alloys Compd. 491 (2010) 200–202.
[21] J. She, Y.Z. Zhan, C.L. Li, et al., J. Alloys Compd. 503 (2010) 57–60.
[22] M.J. Pang, Y.Z. Zhan, W.C. Yang, et al., J. Alloys Compd. 508 (2010) 79–84.
[23] P.Sh. Lansman, M.M. Rutman, S.I. Dudkina, Metal Sci. Heat Treatment 32 (8) (1990) 285–288.
[24] G. Cacciamani, S. De Negri, A. Saccone, R. Ferro, Intermetallics 11 (2003) 1135–1151.
[25] T. Wang, Z.P. Jin, J.C. Zhao, J. Phase Equilib. 22 (2001) 544–551.
[26] T.B. Massalski, H. Okamoto, P.R. Subramanian, L. Kacprzak (Eds.), Binary Alloy Phase Diagrams, 2nd edition, ASM International, Metals Park, Ohio, 1990.
[27] A. Tyvanchuk, A. Protsyk, Dopov. Akad. Nauk Ukr. RSR, Ser. B 11 (1982) 62–64.
[28] T.B. Massalski, H. Okamoto, P.R. Subramanian, L. Kacprzak (Eds.), Binary Alloy Phase Diagrams, 2nd edition, ASM International, Metals Park, Ohio., 1990.
[29] P. Villars, Pearson's Handbook of Crystallographic Data, ASM International, Materials Park, OH, 1997.
[30] Y. Zhan, Y. Du, Y. Zhuang, Determination of phase diagrams using equilibrated alloys, in: J.C. Zhao (Ed.), Methods for Phase Diagram Determination, 1st edition, Elsevier Science Press, Amsterdam, The Netherlands, 2007, pp. 108–150.
[31] K.H.J. Buschow, A.S. van der Goot, J. Less Common Met. 24 (1971) 117–120.
[32] D.R. Askeland, P.P. Phulé, the Scicence and Engineering of Materials (with CD-ROM), Fourth edition, CaRIne Crystallography 3.1 for Students, Thomson Brooks/Cole, 2003.
[33] I. Pop, N. Dihoiu, L. Pop, Physica 31 (1986) 32–35.
[34] H. Zhou, W. Liu, S. Yuan, et al., J. Alloys Compd. 336 (2002) 218–221.
[35] P.L. Qin, Z.P. Xu, Z.L. Qin, et al., J. Alloys Compd. (2011), doi:10.1016/j.jallcom.2011.01.080.
[36] H. Okamoto, J. Phase Equilib. 23 (2002) 455–456.
[37] V. Rigaud, B. Sundman, D. Daloz, G. Lesoult, CALPHAD 33 (2009) 442–449.